Biophys. Struct. Mechanism 3, 207–227 (1977)

Biophysics of Structure and Mechanism

Mössbauer and Susceptibility Experiments on Different Compounds of Fe^{3+}-Myoglobin

U. F. Thomanek, F. Parak, S. Formanek, and G. M. Kalvius

Physik Department, Technische Universität München,
James-Franck-Straße, D-8046 Garching, Federal Republic of Germany

Abstract. The static magnetic susceptibilities of different ferric high spin and low spin compounds of myoglobin ($Mb(H_2O)$, $Mb(H_2O)$ frozen under high pressure, MbF, MbCN) were measured in the temperature region between 4.2 K and 130 K. Mössbauer absorption experiments on $Mb(H_2O)$ and MbF were performed at different temperatures between 4.2 K and 180 K and in small magnetizing fields $H \leq 1$ kOe. The evaluation of our experimental data was performed with a Hamiltonian describing the $3d^5$-configuration of the ferric iron by taking into account the Coulomb repulsion of the five electrons within the $3d$-shell, the crystal electric field of C_{2v}-symmetry, and the spin-orbit coupling. The Hamiltonian contains the splitting energies of the five antibonding d-orbitals (d_{xy}, d_{xz}, d_{yz}, $d_{x^2-y^2}$, d_{z^2}) as parameters. The values of these energies were obtained by a least squares fitting procedure using our magnetic susceptibility data together with the g-factors taken from the literature. In the case of MbF the energy difference between the two lowest Kramers doublets was also determined from present Mössbauer data. The results of the susceptibility and the Mössbauer data are in good agreement.

The splitting energies of the $3d$-orbitals can be correlated to the distances between the iron and its nearest neighbours. The different positions of the iron in the compounds investigated are discussed.

Key words: Mössbauer — Susceptibility — Fe^{3+} — Myoglobins.

1. Introduction

The O_2 binding mechanism of various hemoglobins has been studied in some detail by several different experimental methods. Although X-ray structure investigations have brought deep insight into the functional properties of hemoglobin, spectroscopic methods have become more and more important recently. In contrast to the X-ray structure determination the spectroscopic methods are only sensitive to certain well-defined places within the molecule. Much attention has been paid to the properties of

the iron atom and its immediate surroundings, since it represents the active center of all hemoglobins to which the O_2 molecule may be bound.

During the past years a large number of experimental and theoretical papers have been published concerning the determination of the electronic structure of the iron in various Fe^{2+}-hemeproteins (Eicher et al., 1969; Eicher et al., 1975; Trautwein, 1975). A comparison of the different electronic structures may help to understand the mechanism which controls the O_2-affinity. It should be emphasized that the dynamical behaviour of the protein can be inferred from these investigations only rather indirectly since all experiments are performed on samples in which the molecules are frozen into a static state. More detailed information about the dynamical behaviour of the binding mechanisms can be obtained only from dynamical experiments (Frauenfelder, 1975). It has been shown (Eicher et al., 1969; Eicher et al., 1975) that it is possible to calculate the eigenvalues and the eigenvectors of the energetically low-lying states of the electronic term scheme of the ferrous iron in deoxygenated myoglobin and hemoglobin using a crystal field approach. In these calculations a Hamiltonian containing a certain number of free parameters is diagonalized which involves the Coulomb repulsion of the $3d$ electrons, the interaction of these electrons with a crystal electric field of C_{2v} symmetry and the spin-orbit coupling. The values of these parameters which are equal to the crystal field splitting of the antibonding $3d$ electron orbitals have to be determined from the experiment. The temperature dependence of the quadrupole splitting of deoxygenated myoglobin and hemoglobin measured by Mössbauer spectroscopy can be used for this purpose. Although the Fe^{2+}-hemoglobins are of particular interest, since O_2 is stored or transported only when the iron is in the ferrous state, a great number of spectroscopic investigations have been performed as well on hemoglobins in which the iron is in the Fe^{3+} state (Perutz et al., 1974a; Perutz et al., 1974b; Perutz et al., 1974c). In the present work we investigated various ferric compounds of myoglobin by Mössbauer spectroscopy and by susceptibility measurements. The evaluations were also done by means of a crystal field model. The Hamiltonian which contains the different interactions acting on the $3d$ electrons within the $3d^5$-configuration, is constructed in analogy to the one used in the case of ferrous compounds of myoglobin and hemoglobin (Eicher et al., 1969; Eicher et al., 1975). A detailed description of this procedure is given by Eicher (1975). In contrast to the results of the deoxygenated hemeproteins mentioned above it was not possible to infer the electronic structure of the ferric iron exclusively from the evaluation of the Mössbauer spectra at different temperatures between $T = 4.2$ K and $T = 200$ K. The Mössbauer spectra of high spin ferric compounds show only a very small temperature dependence of the quadrupole splitting because of the spherical symmetry of the electronic ground state ($^6A_1$) and because of the very low thermal population of higher electronic levels, which contribute to the electric field gradient. Furthermore, the mixing of these higher electronic levels, to the ground state by spin-orbit coupling proved to be rather small. An additional experimental difficulty is that the Mössbauer spectra of a number of ferric compounds of hemeproteins become indistinct in a temperature range between $T = 10$ K and $T = 200$ K since paramagnetic relaxation effects are dominant.

Presently we are not able to fit appropriate theoretical curves to these relaxation spectra. Nevertheless, it is possible to extract much useful information about the

electronic structure of the ferric iron by the Mössbauer absorption spectra at low temperatures and by a qualitative comparison of the relaxation spectra of different samples, as will be discussed later. Therefore in addition we measured the static magnetic susceptibility between $T = 4.2$ K and $T = 130$ K of some ferric compounds of myoglobin. In order to determine the free parameters of the Hamiltonian, which describes the electronic system of the $3d^5$-configuration, the experimental data were compared in least squares fitting procedures with the theoretical magnetization curves which can easily be computed from the electronic term scheme. To evaluate the free parameters without ambiguity it was necessary to use the g-factors (Gray et al., 1973; Horrocks et al., 1974) of the lowest Kramers doublet known from EPR experiments as an additional information.

Some years ago the magnetic susceptibility of a metmyoglobin and a myoglobin-fluoride sample was measured at low temperatures by a Japanese group (Tasaki et al., 1967). They tried to fit their data by means of a Spin Hamiltonian. However, the theoretical curves obtained showed significant deviations from the experimental data. Because the Spin Hamiltonian does not take into account the mixing of the wave functions of the energetically higher states to the ground state by spin-orbit coupling, we believe that the interpretation used in the present work is more appropriate. Furthermore, one is met with some difficulties, if one tries to correlate the parameters of the Spin Hamiltonian with other physical and chemical properties of the system. The free parameters used in the present work are the splitting energies of the antibonding single $3d$ electron orbitals. Changes of these energies can be correlated to different spatial arrangements of the iron relative to its nearest neighbours in a straight forward manner. Information about any differences concerning the spatial arrangements of the iron in different hemeproteins are highly important for discussions of structural changes on ligand binding in hemeproteins.

2. Theory

The Electronic Structure of the Ferric Iron

For the calculation of the energies of the low-lying electronic levels as a function of a set of free parameters we used the theory developed by Eicher (1975). In this approach the total Hamiltonian ($\hat{H}$) contains four parts which take into consideration the Coulomb repulsion ($\hat{H}_{Cb}$) of the five $3d$ electrons, a crystal electric field ($\hat{H}_{C_{4v}}$) of tetragonal symmetry, a rhombic distortion ($\hat{H}_{\text{rhom}}$) of the tetragonal symmetry of the crystal electric field and the spin-orbit coupling ($\hat{H}_{LS}$).

$$\hat{H} = \hat{H}_{Cb} + \hat{H}_{C_{4v}}(\varepsilon_1, \varepsilon_2, \varepsilon_3) + \hat{H}_{\text{rhom}}(D, E) + \hat{H}_{LS}(\xi) \tag{1}$$

ε_1, ε_2, ε_3, D and E are free parameters which had to be determined by comparison with the experimental data. The definition of ε_1, ε_2 and ε_3 as the splitting energies of the antibonding $3d$ orbitals caused by the crystal electric field can be seen from Figure 1. The parameters D and E determine the rhombic distortion of the crystal electric field, the symmetry of which is assumed to be C_{4v} in first order. The energy splitting of the initially degenerated d_{xz} and d_{yz} orbitals caused by $\hat{H}_{\text{rhom}}$ is exactly

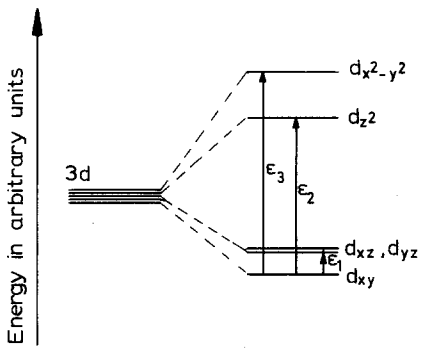

Fig. 1. Splitting of the five $3d$-orbitals caused by a crystal electric field of C_{4v}-symmetry

$2 \cdot (D + E)$. The spin-orbit coupling constant ξ has been taken equal to 300 cm^{-1} corresponding to the consideration of Eicher (1975).

Since the diagonalization of $\hat{H}$ as given by Equation (1) within the $3d^5$ configuration is practically impossible, in a first step only the Hamiltonian

$$\hat{H}_1 = \hat{H}_{Cb} + \hat{H}_{C_{4v}}(\varepsilon_1, \varepsilon_2, \varepsilon_3) \tag{2}$$

is diagonalized within the basis set of the $3d^5$ configuration, consisting of all possible five-electron multiplets ${}^{(2S+1)}_{\alpha}L$. (Here $(2S + 1)$ is the spin multiplicity, L is the angular momentum and α is the seniority number). It was shown that the ${}^4A_2$, ${}^2E$, ${}^2B_2$, ${}^4E$, and the ${}^6A_1$-level always have the lowest energies, if the calculations are carried out with realistic ε-values. Thus one may reasonably expect that only these five states determine the spectroscopic properties of the $3d^5$ configuration of the iron with respect to Mössbauer, susceptibility, and EPR data. The remaining states will therefore not be taken into account in the following computations.

Within the range given by

$$\begin{aligned} &22000 < \varepsilon_3 < 28000 \\ &0.4\ \varepsilon_3 < \varepsilon_2 < 0.8\ \varepsilon_3 \\ &-200 < \varepsilon_1 < 800 \end{aligned} \tag{3}$$

linear relations between ε_1, ε_2, ε_3 and the energies of the low-lying levels $E({}^4A_2)$, $E({}^2E)$, $E({}^2B_2)$ and $E({}^4E)$ were inferred as follows:

$$\begin{aligned} E({}^6A_1) &= 0 \qquad \text{(reference level)} \\ E({}^4A_2) &= 24765 - 0.99 \cdot \varepsilon_3 \\ E({}^2E) &= 36960 - 0.96 \cdot \varepsilon_1 - 0.93 \cdot \varepsilon_2 - 0.98 \cdot \varepsilon_3 \\ E({}^2B_2) &= 37570 + 1.90 \cdot \varepsilon_1 - 0.98 \cdot \varepsilon_2 - 0.96 \cdot \varepsilon_3 \\ E({}^4E) &= 26480 + 0.96 \cdot \varepsilon_1 - 0.12 \cdot \varepsilon_2 - 0.85 \cdot \varepsilon_3 \end{aligned} \tag{4}$$

The energies are given in units of cm^{-1}. The ranges chosen in Equation (3) cover the ε-values obtained in the present investigations.

The next step is to diagonalize the total Hamiltonian $\hat{H}$ of Equation (1) using the levels ${}^6A_1$, ${}^4A_2$, ${}^2E$, ${}^2B_2$, ${}^4E$ as basis vectors. Because of the multiplicity of these levels

one obtains twelve eigenvalues E_ν and eigenvectors $|\nu\pm\rangle$ which depend on the free parameters ε_1, ε_2, ε_3, D and E. These twelve eigenvectors $|\nu\pm\rangle$ still are twofold degenerate (Kramers doublets). The energy differences between the Kramers doublets $E_\nu - E_1$ (the energy E_1 is assumed to be the lowest one) shall be designed by $\Delta_{\nu-1}$.

Determination of the Free Parameters of the Hamiltonian $\hat{H}$ from Susceptibility and g-Factor Measurements

The 12 wavefunctions $|\nu\pm\rangle$ and their energies (E_ν or the differences Δ_ν) are completely determined by the parameters ε_1, ε_2, ε_3, D and E. These parameters have to be obtained experimentally. Since we used for this purpose the temperature dependence of the paramagnetic magnetization and the g-factors, it is necessary first to calculate the influence of an external magnetizing field $\vec{\mathbf{H}}(\vartheta, \varphi)$ to the energies and wavefunctions of the electronic system.

The g-factors of the individual Kramers doublets $|\nu\pm\rangle$ are calculated from the first order perturbation energies of the Hamiltonian $\hat{H}_{\text{magn}}$ which has to be added to the total Hamiltonian $\hat{H}$ of Equation (1):

$$\hat{H}_{\text{magn}} = \beta \cdot \vec{\mathbf{H}}(\vartheta, \varphi) \cdot (\vec{\mathbf{L}} + g_s \cdot \vec{\mathbf{S}}) . \tag{5}$$

Here β is the Bohr magneton, and $g_s = 2.0023$ is the g-factor of the free electron spin.

The energy splittings $\Delta\delta'_\nu(\vartheta, \varphi)$ of the Kramers doublets $|\nu\pm\rangle$ caused by the magnetizing field $\vec{\mathbf{H}}(\vartheta, \varphi)$ are the differences of the eigenvalues $\delta'_{\nu+}(\vartheta, \varphi)$ and $\delta'_{\nu-}(\vartheta, \varphi)$ of the matrix:

$$\begin{pmatrix} \langle \nu+|\hat{H}_{\text{magn}}|\nu+\rangle & \langle \nu+|\hat{H}_{\text{magn}}|\nu-\rangle \\ \langle \nu-|\hat{H}_{\text{magn}}|\nu+\rangle & \langle \nu-|\hat{H}_{\text{magn}}|\nu-\rangle \end{pmatrix}. \tag{6}$$

The g-factors $g_\nu(\vartheta, \varphi)$ of the individual Kramers doublets may be computed as follows:

$$g_\nu(\vartheta, \varphi) = \frac{\Delta\delta_\nu'(\vartheta, \varphi)}{\beta \cdot |\vec{\mathbf{H}}|} . \tag{7}$$

Since the wave functions of the Kramers doublets $|\nu\pm\rangle$ are functions of the free parameters ε_1, ε_2, ε_3, D and E, the g-factors $g_\nu(\vartheta, \varphi)$ will also depend on these parameters. The terms of second order perturbation theory will not change the g-factors. In contrast to the approach used by Eicher (1975) the terms of higher order are neglected, because the g-factors used in our evaluations had been measured at relatively low magnetic fields (Gray et al., 1973; Horrocks et al., 1974).

In the computations of the induced paramagnetic magnetizations $M_{\nu\pm}(\vartheta, \varphi)$ of the individual levels, however, the terms of second order perturbation theory must be considered too. The energy shifts in second order $\delta''_{\nu\pm}(\vartheta, \varphi)$ of the levels $|\nu\pm\rangle$ may be written as follows:

$$\delta''_{\nu\pm} = \sum_{\substack{\mu=1 \\ \mu\neq\nu}}^{12} \frac{|\langle\mu'+|\,\hat{H}_{\text{magn}}|\,\nu'\pm\rangle|^2 + |\langle\mu'-|\,\hat{H}_{\text{magn}}|\nu'\pm\rangle|^2}{E_\nu - E_\mu}. \tag{8}$$

The wave functions $|\nu'\pm\rangle$ ($\nu = 1, 2, 3 \ldots 12$) are the eigenvectors of the matrix given in Equation (6). The energies E_ν are the eigenvalues of the Hamiltonian $\hat{H}$ in Equation (1). Taking into account all terms up to second order the total energies $E^{(2)}_{\nu\pm}$ of the individual levels $|\nu\pm\rangle$ or $|\nu'\pm\rangle$ respectively, are given by:

$$E^{(2)}_{\nu}{}_{\pm}(\vartheta, \varphi) = E_\nu + \delta'_{\nu\pm}(\vartheta, \varphi) + \delta''_{\nu}{}_{\pm}(\vartheta, \varphi)\,. \tag{9}$$

The magnetizations of the individual levels $M_{\nu\pm}(\vartheta, \varphi)$ are computed by:

$$M_{\nu\pm}(\vartheta, \varphi) = -\frac{\partial E^{(2)}_{\nu\pm}(\vartheta, \varphi)}{\partial|\vec{\mathbf{H}}|}. \tag{10}$$

The average value of the magnetization of the Fe^{3+} ion $\langle M(\vartheta, \varphi)\rangle_T$ at a certain temperature T may be calculated inserting the Boltzmann distribution function.

$$\langle M(\vartheta, \varphi)\rangle_T = \frac{\sum_{\nu=1}^{12} (M_{\nu+} \cdot e^{-E^{(2)}_{\nu+}/kT} + M_{\nu-} \cdot e^{-E^{(2)}_{\nu-}/kT})}{\sum_{\nu=1}^{12} (e^{-E^{(2)}_{\nu+}/kT} + e^{-E^{(2)}_{\nu-}/kT})}. \tag{11}$$

For the comparison with the experimental data which had been measured with randomly oriented molecules one has to average over ϑ and φ:

$$\langle M\rangle_T = \tfrac{1}{3}(\langle M(90°, 0°)\rangle_T + \langle M(90°, 90°)\rangle_T + \langle M(0°, \varphi)\rangle_T)\,. \tag{12}$$

Comparing the experimentally determined magnetizations M_{exp} with the theoretical expression above, one may use the relation:

$$\frac{M_{\text{exp}}}{H} = N \cdot \frac{\langle M\rangle_T}{H} + \frac{M_{\text{dia}}}{H}, \tag{13}$$

where H is equal to the magnitude of the magnetizing field $|\vec{\mathbf{H}}|$, N is the number of paramagnetic iron ions in the sample and M_{dia} is the diamagnetic magnetization of the whole sample including the sample holder and the salt solution. N is determined by means of optical spectroscopy (see part 3), whereas M_{dia} is an additional fitting parameter.

Using Equation (13) the unknown parameters $E(^4A_2)$, $E(^2E)$, $E(^2B_2)$, D, E and M_{dia} could be determined in principle by a least squares fitting procedure. Which of these six free parameters actually could be determined by the fitting routine shall be discussed later. Because of their linear dependence [see Equation (4)] it is possible to use either the energies ε_1, ε_2, and ε_3 or the energies $E(^4A_2)$, $E(^2E)$ and $E(^2B_2)$ as free parameters.

Calculation of the Low Temperature Mössbauer Spectra

The energy differences between the resonance lines appearing in the Mössbauer spectra of our samples arise from the hyperfine interactions. These energies are in

the order of 10^{-2} cm^{-1}, which is much less than the energy differences between the different Kramers doublets. That means that the Hamiltonian describing the hyperfine interactions may be treated as a small perturbation of the total Hamiltonian $\hat{H}$ of Equation (1). A mixing of different Kramers doublets with each other by means of the hyperfine interactions is not to be expected. A mixing of the two levels of a Kramers doublet due to the hyperfine interactions can also be avoided, if one applies a small magnetizing field $\vec{\mathbf{H}}$ of about 1 kOe to the sample. Consequently the interaction between the electronic shell and the atomic nucleus may be treated separately for each electronic level.

The Hamiltonians $\hat{H}_{\mathrm{NGR}}$ or $\hat{H}^*_{\mathrm{NGR}}$ determining the splitting energies of the ground state and of the first excited state of the ^{57}Fe nucleus respectively, can then be written as:

$$\begin{aligned}\hat{H}_{\mathrm{NGR}} &= \hat{H}_{\mathrm{magn}} + \hat{H}_{\mathrm{mhf}} + \hat{H}_{\mathrm{eq}} - \vec{\mu}_n \cdot \vec{\mathbf{H}} \\ \hat{H}^*_{\mathrm{NGR}} &= \hat{H}_{\mathrm{magn}} + \hat{H}^*_{\mathrm{mhf}} + \hat{H}^*_{\mathrm{eq}} - \vec{\mu}^*_n \cdot \vec{\mathbf{H}}\,. \end{aligned} \tag{14}$$

The definition of $\hat{H}_{\mathrm{magn}}$ has already been given in Equation (5). $\vec{\mu}_n$ and $\vec{\mu}^*_n$ are the nuclear magnetic moments of the ground state and of the 14.4 keV excited state of Fe^{57}, respectively. $\hat{H}_{\mathrm{mhf}}$ and $\hat{H}^*_{\mathrm{mhf}}$ describe the magnetic hyperfine interaction, whereas $\hat{H}^*_{\mathrm{eq}}$ determines the electric quadrupole interaction. For the ground state of the nucleus $\hat{H}_{\mathrm{eq}}$ vanishes and for the 14.4 keV level $\hat{H}^*_{\mathrm{eq}}$ is given by:

$$\hat{H}^*_{\mathrm{eq}} = \frac{e \cdot Q \cdot V_{zz}}{4 \cdot I \cdot (2\,I - 1)} \cdot (3\,I_z^2 - I(I+1))\,, \tag{15}$$

where e is the elementary charge, Q is the nuclear electric quadrupole moment, V_{zz} is the electric field gradient of the nucleus in the direction of the z-axis and I is the nuclear spin. In Equation (14) and (15) the point symmetry of the iron is assumed to be C_{4v} which should be a good enough approximation for the evaluation of the Mössbauer spectra, as the experimental g-factors g_x and g_y of metmyoglobin and metmyoglobin fluoride differ only slightly.

The operators $\hat{H}_{\mathrm{mhf}}$ and $\hat{H}^*_{\mathrm{mhf}}$ may be written in a very simple form, if one takes into account that the orbital angular momentum $\vec{\mathbf{L}}$ is strongly quenched by the interaction of the crystal electric field ($\hat{H}_{C_{4v}}$) and by the spin-orbit coupling ($\hat{H}_{LS}$). By the application of the Wigner-Eckart theorem one can show, that

$$\begin{aligned}\hat{H}_{\mathrm{mhf}} &= g_n \cdot A_0 \cdot \vec{\mathbf{S}} \cdot \vec{\mathbf{I}} \\ \hat{H}^*_{\mathrm{mhf}} &= g^*_n \cdot A_0 \cdot \vec{\mathbf{S}} \cdot \vec{\mathbf{I}} \end{aligned} \tag{16}$$

g_n and g^*_n are the nuclear g-factor of the two nuclear levels involved. A_0 is the hyperfine coupling constant which is the same for both nuclear levels.

For the computation of the eigenvalues and eigenvectors of $\hat{H}_{\mathrm{NGR}}$ and $\hat{H}^*_{\mathrm{NGR}}$ a set of basis vectors was used which are composed of an electronic part ($|\nu' \pm\rangle$) and of a nuclear part ($|I, I_z\rangle$).

It has already been mentioned, that due to relaxation processes only the spectra at low temperatures could be fitted by the theory described here. For that reason only the ground state Kramers doublet $|1' \pm\rangle$ which is split into two singlets by $\hat{H}_{\mathrm{magn}}$ is taken into account. The second Kramers doublet $|2' \pm\rangle$ separated from $|1' \pm\rangle$

by the energy Δ_1 has to be considered only in the case of MbF, as will be discussed later on.

It should be remembered that the eigenvalues and the eigenvectors of the Hamiltonians $\hat{H}_{\mathrm{NGR}}$ and $\hat{H}^*_{\mathrm{NGR}}$ are still functions of the angle ϑ, which is the angle between the C_{4v} axis and the direction of the applied magnetizing field $\vec{\mathbf{H}}$.

The isomer shift of our samples is treated as a constant parameter, which had to be added to the calculated energies of the resonance lines. Thus we have three parameters which have to be determined by fitting the Mössbauer spectra. They are: the magnetic hyperfine coupling constant A_0, the electric quadrupole splitting $\frac{1}{2} \cdot e \cdot Q \cdot V_{zz}$ and the isomer shift S. In principle the parameters ε_1, ε_2 and ε_3 which determine the g-factors of the Kramers doublets could also be regarded as free parameters in such a fit. For the sake of simplicity we have used the g-factors of the lowest Kramers doublet as taken from the literature (Gray et al., 1973).

For the computation of the shape of the spectra it is also necessary to calculate the relative intensities of the individual resonance lines. For this the following formula was used (DeBennedetti, 1964):

$$P(\vartheta; \tfrac{3}{2}, l; \tfrac{1}{2}, k) = \Big|\sum_{i,j} u(i, k) \cdot v(j, l) \cdot M(I_{z,j}, I_{z,i})\Big|^2 \tag{17}$$

The indices k and l number the eigenvalues of $\hat{H}_{\mathrm{NGR}}$ and of $\hat{H}^*_{\mathrm{NGR}}$, respectively. The coefficients $u(i, k)$, $(i = 1, 2)$ and $v(j, l)$, $(j = 1, 2, 3, 4)$ define the eigenvectors of the nuclear levels. $M(I_{z,j}\, I_{z,i})$ is given by:

$$M(I_{z,j}, I_{z,i}) = \langle \tfrac{1}{2}, I_{z,i}; L = 1, M | \tfrac{3}{2}, I_{z,j} \rangle \cdot X^M_{L=1} \tag{18}$$

and

$$M = I_{z,j} - I_{z,i}\,.$$

The vectors $X^M_{L=1}$ describe the angular dependence of a $M1$ γ-radiation.

$$X^1_1 = \tfrac{1}{2}\sqrt{2}\begin{pmatrix} -1 \\ i \cdot \cos\vartheta \end{pmatrix}, \quad X^0_1 = \begin{pmatrix} 0 \\ i \cdot \sin\vartheta \end{pmatrix}, \quad X^{-1}_1 = -\tfrac{1}{2}\sqrt{2}\begin{pmatrix} 1 \\ i \cdot \cos\vartheta \end{pmatrix}. \tag{19}$$

Here ϑ is the angle between the direction of the γ-ray and the C_{4v} axis of the iron site (z-axis). Since in our experiments a geometrical arrangement was used, in which the direction of the applied magnetizing field $\vec{\mathbf{H}}$ was always parallel to the direction of the γ-ray (longitudinal field) the angle ϑ here is identical with the one used earlier in Equation (5). As our experiments have been performed on isotopic samples, one has to average over the angle ϑ. Therefore we calculated the spectra for $\vartheta = 0°$, $3°$, $6° \ldots 180°$ and added them up multiplying each of them by the weighting factor $\sin\vartheta$.

3. Sample Preparation and Experimental Techniques

Sample Preparation

For the magnetization measurements we exclusively used polycrystalline material in order to get a high concentration of the individual myoglobin derivatives in our samples. The volume of the sample holders, amounts to about 50 mm^3. The prepara-

tion and the crystallization of sperm whale metmyoglobin $Mb(H_2O)$ in a 3.75 molar $(NH_4)_2SO_4$-solution at pH = 6.3 was done according to the procedures described by Kendrew and Parrish (1956). The MbCN and the MbF derivatives were obtained by adding KCN, respectively NaF to the $(NH_4)_2SO_4$-solution, in which the $Mb(H_2O)$ crystals had been crystallized. Before filling the myoglobin crystals into the sample holders the crystals were broken to very small pieces by a glass rod in order to avoid any anisotropy effects in the measurements. Afterwards the samples were frozen by insertion into liquid nitrogen. Besides the three derivatives $Mb(H_2O)$, MbCN and MbF mentioned above we also investigated a metmyoglobin sample, which was cooled to 77 K by a special freezing method. It is possible to avoid the usually occuring destructions of the crystal lattice of a myoglobin single crystal during its freezing by appliying a hydrostatic pressure of about 2500 atm (Thomanek et al., 1973). X-ray structure investigations of metmyoglobin single crystals frozen under these conditions showed no significant structural changes of the molecule (Parak et al., 1975). Especially in the environment of the iron no structural change could be detected. In the investigations of a metmyoglobin sample frozen at the hydrostatic pressure of 2500 atm $(Mb(H_2O)_{p\text{-Ice}})$ we looked for changes in the electronic structure of the iron ion. The magnetization measurements of this sample $(Mb(H_2O)_{p\text{-Ice}})$ could be carried out at atmospheric pressure, because the structure of this special ice phase is metastable for long times at temperatures below $T = 100$ K.

By Mössbauer spectroscopy we investigated solutions of metmyoglobin and myoglobin fluoride. In order to get appreciable absorption effects we exclusively used samples enriched with ^{57}Fe. The procedures for the chemical enrichment of the natural sperm whale myoglobin molecules are described elsewhere (Parak et al., 1971). The amount of myoglobin in our samples was about 60—70 mg dissolved in $(NH_4)_2SO_4$-solutions of various concentrations. Their values will be given later for the individual samples.

Magnetization Measurements

Magnetizations were measured by a vibrating sample magnetometer with superconducting magnets (Princeton Applied Research Corporation, Model 150A). The physical and technical principles of such magnetometers have been described, for example, by Feldmann et al. (1964).

The sample can be vacuum insulated from the vessel containing the liquid helium. Thus it is possible to measure magnetizations not only at $T = 4.2$ K but also at temperatures between $T = 12$ K and room temperature. As our temperature sensor (GaAs diode) could not be fixed directly at the sample but was thermally coupled to the sample via the helium exchange gas a very careful calibration was necessary. For the temperature calibration we used calibrated platinum and germanium resistance thermometers.

The measurements of the high-spin compounds of myoglobin have been carried out at a magnetizing field of $H = 10.0 \pm 0.02$ kOe, whereas for myoglobin cyanide $H = 20.0 \pm 0.04$ kOe were used. At $H = 10.0$ kOe the experimentally determined magnetic moments of the high spin compounds at $T = 4.2$ K were in the order of about 10^{-2} emu, whereby our samples contained about $1 \cdot 10^{18}$—$2 \cdot 10^{18}$ protein

molecules. The maximum sensitivity achieved with our apparatus was about $3 \cdot 10^{-5}$ emu. The number of myoglobin molecules contained in a sample was determined after the magnetization measurements. For this purpose we dissolved our samples in 50 or 100 ml of water and measured the intensities of the absorption maxima at the characteristic wave lengths of the different compounds in the range from 410–600 nm (Antonini et al., 1971). In addition, the samples were also analyzed quantitatively after converting them to reduced pyridine hemochromogen. Absorption measurements of these hemochromogen solutions were carried out at 540 nm and 557.5 nm. At these wavelengths the absorption coefficients are $\varepsilon_{540} = 9000 \frac{\text{liter}}{\text{cm} \cdot \text{mole}}$, $\varepsilon_{557.5} = 32000 \frac{\text{liter}}{\text{cm} \cdot \text{mole}}$, as taken from DeDuve (1948). The accuracy in the determination of the number of iron ions was about $\pm 1\%$.

Mössbauer Absorption Spectra

The Mössbauer measurements were carried out in a liquid helium cryostat equipped with a superconducting solenoid (Siemens, Model Kryos 180). In order to vary the temperature of the absorber between $T = 4.2$ K and room temperature, a second small cryostat was constructed which was inserted into the bore of the solenoid. The small cryostat can be vacuum insulated from the surrounded liquid helium bath and the temperature of the sample can be raised up to room temperature by a small heater without causing any considerable increase in the consumption of liquid helium. The temperature sensor used here was a Si-diode (D446, Texas Instruments). In our temperature calibration we achieved an accuracy of ± 0.5 degrees.

^{57}Co diffused into a rhodium matrix was used as the source. The temperature of the source was the same as the absorber temperature. It had been shown in test experiments that the width of emission line of this source is practically temperature independent. A sinusoidally operating electromechanical Mössbauer spectrometer was used. Data were stored in 400 channel analyzer (Laben Spectroscope, Model 400) in time mode. Synchronization of velocity and time sweep was performed according to Kaindl et al. (1968). The 14.4 keV gamma quanta were detected by a proportional counter filled with 96% argon and 4% CO_2.

4. Evaluation and Results

Susceptibility Measurements

As already mentioned, we used the energies of the $^4A_2$-, ^2E- and $^2B_2$-levels relative to the $^6A_1$-level, the rhombic distortion energies D and E, and the diamagnetic contribution M_{dia} as parameters in the least squares fitting procedures. It turned out, that only two or three of these six parameters could be determined reliably by the least squares fits of the susceptibility data. These are the diamagnetic contributions M_{dia} and in the case of high spin compounds the energies $E(^4A_2)$ and $E(^2E)$, if $E(^2E) < 15000$ cm^{-1}. If the energy $E(^2E)$ is greater than 1500 cm^{-1} the accuracy of its

determination is very low, because the influence of the ^2E state to the magnetic properties of the iron at low temperatures becomes very small. The remaining parameters $E(^2B_2)$, D and E have either to be determined by other experimental methods or have to be fixed at reasonable values. For that reason we used the experimental g-factor of the lowest Kramers doublet ($g_\perp = 1/2(g_x + g_y)$ and $g_{xy} = g_x - g_y$) taken from the literature as additional data. Thereby the accuracy of the determination of $E(^2E)$ became much better and one of the parameters D or E could then also be determined. We did not use the g-factors as further experimental data in our fitting procedure, but rather fitted only the susceptibility data using $E(^4A_2)$ and M_{dia} as free parameters and then varying the energies $E(^2E)$ and D step by step within a certain range. The parameters $E(^2B_2)$ and E were kept at constant values which will be discussed later. In this manner we got a series of slightly different electronic level schemes all of which gave the correct susceptibility data but show small differences in the g-factor of the ground state Kramers doublet. As the final result we took that electronic term scheme, which showed the best agreement with the experimental g-factors.

As mentioned above the energies $E(^2B_2)$ and E had to be fixed at constant values. In contrast to the calculation of Eicher (1975) we set $E = 0\ \text{cm}^{-1}$. As may be seen from Figure 2 in (Eicher, 1975), it is purely optional to fix the energy E at a certain value and then use D as a fitting parameter, since the two parameters D and E are linearly dependent on each other. Setting $E = 0\ \text{cm}^{-1}$ corresponds to the approach used earlier for Fe^{2+}-Myoglobin (Eicher et al., 1975). The energy $E(^2B_2)$ had been fixed by keeping the energy difference $(E(^2B_2) - E(^2E))$ at a constant value. From the Equation (4) it may be seen that this energy difference is mainly deter-

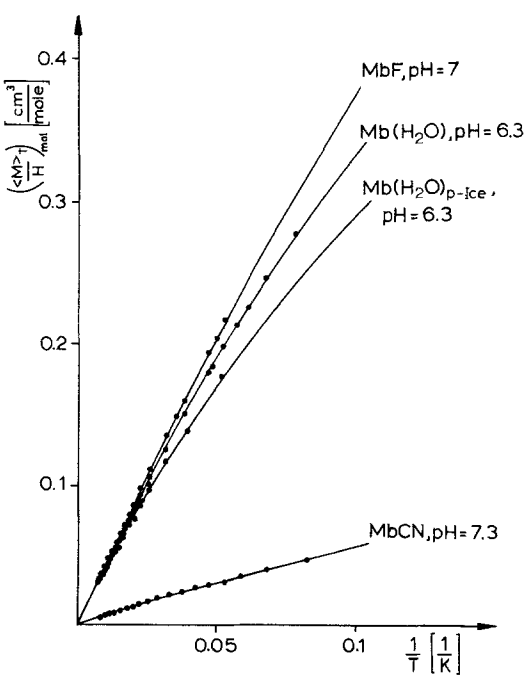

Fig. 2. Experimental results of the magnetization measurements at different temperatures and constant magnetizing fields $\vec{H}$. The solid curves are obtained from the least squares fitting procedures taking into account also the experimental data at $T = 4.2$ K which are not shown in the figure

mined by the energy ε_1, which lies in the order of a few hundreds of cm^{-1}. Therefore we set:

$$E(^2B_2) - E(^2E) = 500\ cm^{-1}.$$

Alterations of this value modifies the energy ε_2 only slightly [see Equation (4)]. This uncertainty was taken into account in the error bars of ε_2. Consequently the energy ε_1 cannot be determined by the evaluation of our data, whereas the energies ε_2 and ε_3 may be calculated from the energies $E(^4A_2)$ and $E(^2E)$ via the Equation (4). Fortunately the energies ε_2 and ε_3 contain the most relevant information about the spatial arrangement of the iron relative to its nearest neighbours.

In Figure 2 the temperature dependence of the ratio of experimental magnetizations M_{exp} and the applied magnetizing field H, corrected for the diamagnetic part M_{dia} and calculated for one mole of the substances are shown together with the theoretical curves, which have been obtained in the least squares fitting procedures. The temperature scale of Figure 2 makes it impossible to show the data at 4.2 K. They are in very good agreement with the theoretical values as well and have also been taken into account in the fitting procedures. In Table 1 we summarize our results of the magnetization measurements of the individual high spin compounds. Since we do not know the g-factors of the lowest Kramers doublet of $Mb(H_2O)_{p\text{-Ice}}$, we set the parameter D equal to 50 cm^{-1}. This gave a reasonable g-factor g_{xy} in comparison to $Mb(H_2O)$. Figures 3 and 4 show the energy diagrams of the levels $^6A_1$, $^4A_2$ and ^2E and of the antibonding single $3d$ electron orbitals d_{xy}, d_{yz}, d_{xz}, d_{z^2} and $d_{x^2-y^2}$ of the individual high spin compounds. Figure 3 also shows the splittings of

Table 1. The energies of the low lying $3d^5$ electron multiplets $^4A_2$, ^2E, $^2B_2$ and ^4E relative to the $^6A_1$ level of the Fe^{3+} ion of some ferric high spin compounds of metmyoglobin. The definition of the energies ε_2 and ε_3 are given in Figure 1. Δ_1 and Δ_2 are the splitting energies of the $^6A_1$ level, the splitting of which is caused by the spinorbit coupling

	$Mb(H_2O)_{p\text{-Ice}}$ (pH = 6.3)	$Mb(H_2O)$ (pH = 6.3)	MbF (pH = 7.0)
$E(^6A_1)$ [cm^{-1}]	0	0	0
$E(^4A_2)$ [cm^{-1}]	667 ± 40	1295 ± 60	1963 ± 80
$E(^2E)$ [cm^{-1}]	1500 ± 500	3500 ± 700	1525 ± 400
$E(^2B_2)$ [cm^{-1}]	2000	4000	2025
$E(^4E)$ [cm^{-1}]	4300 ± 600	4960 ± 600	5340 ± 600
ε_2 [cm^{-1}]	12500 ± 900	10940 ± 1000	13960 ± 800
ε_3 [cm^{-1}]	24342 ± 40	23707 ± 60	23032 ± 80
Δ_1 [cm^{-1}]	30.5 ± 2.0	22.2 ± 1.5	12.7 ± 1.0
Δ_2 [cm^{-1}]	131.3 ± 6.0	72.4 ± 2.0	44.0 ± 2.0
$g_\perp = \frac{1}{2} \cdot (g_x + g_y)$[a]	–	5.92	5.96
$g_{xy} = g_x - g_y$[a]	–	0.13	0.18
D [cm^{-1}]	50	122 ± 30	75 ± 20
$\frac{M_{dia}}{H} \cdot 10^7$ [cm^3]	−1.90 ± 0.04	−0.88 ± 0.015	−1.29 ± 0.02

[a] The g-factors had been taken from Gray et al. (1973)

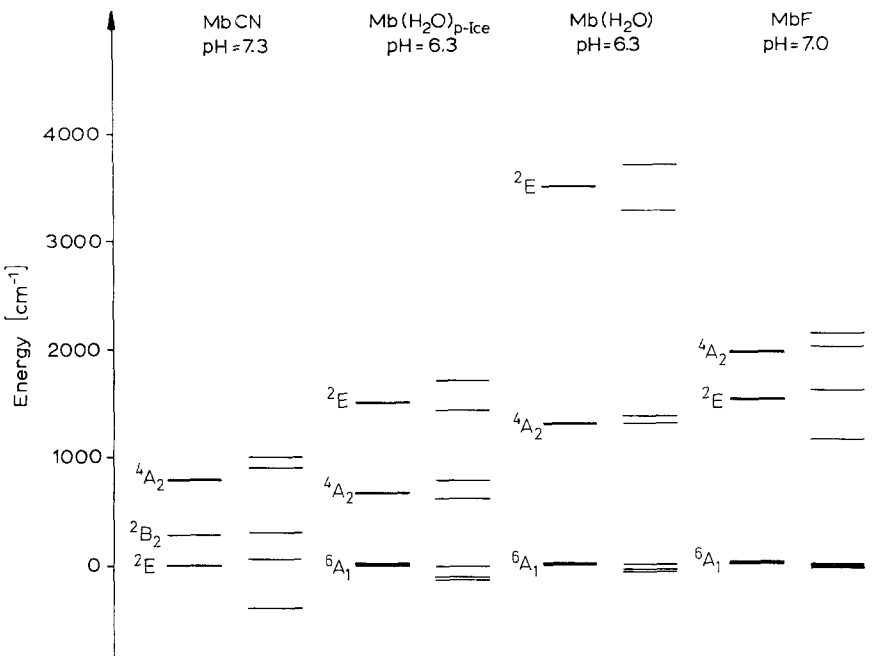

Fig. 3. The energies of the multi-electron levels ${}^6A_1$, ${}^4A_2$ and ${}^2E$ of the ferric iron in different compounds of myoglobin. The energies of the groundstates are set to $E = 0$. The splittings of the multi-electron levels caused by the rhombic distortion of the C_{4v}-symmetry of the crystal field and by the spin-orbit coupling are also shown in the figure

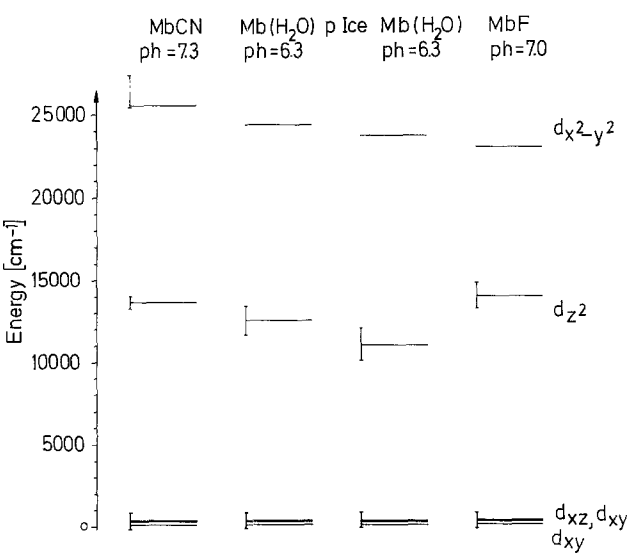

Fig. 4. The energies of the antibonding single $3d$ electron orbitals $d_{x^2-y^2}$, d_{z^2}, d_{xz} and d_{yz} relative to the d_{xy}-orbital. The error bars of the $d_{x^2-y^2}$-orbitals of the high spin compounds are so small, that they cannot be shown in the figure

Table 2. The energies of the low lying $3d^5$ electron multiplets $^6A_1$, $^4A_2$, $^2B_2$ relative to the ^2E level of the Fe^{3+} ion in myoglobin cyanide. Δ_1 and Δ_2 are the energy differences between the three Kramers doublets of the ^2E and $^2B_2$ level

	MbCN (pH = 7.3)
$E(^2E)$ [cm^{-1}]	0
$E(^2B_2)$ [cm^{-1}]	270 ± 50
$E(^4A_2)$ [cm^{-1}]	800 ± 400
$E(^6A_1)$ [cm^{-1}]	1500
ε_2 [cm^{-1}]	13600 ± 500
ε_3 [cm^{-1}]	25500
Δ_1 [cm^{-1}]	450 ± 20
Δ_2 [cm^{-1}]	700 ± 50
g_x[a]	0.93
g_y[a]	1.89
g_z[a]	3.45
D [cm^{-1}]	61 ± 4
$\frac{M_{dia}}{H} \cdot 10^7$ [cm^3]	−0.47 ± 0.01

[a] The g-factors are taken from Horrocks et al. (1974)

the electron multiplets caused by the spin-orbit coupling and by the rhombic distortion of the crystal field.

For the evaluation of the data of myoglobin cyanide we first looked at the g-factors of the lowest Kramers doublet (Horrocks et al., 1974). By a large number of simulations we found that the ^2E level had to be the ground state and the $^2B_2$ term should be the first excited state. The g-factors are mainly determined by the parameter D and by the energy difference $(E(^2E) - E(^2B_2))$, which in this case has to be about 270 cm^{-1}. By fitting our experimental magnetization data we saw, that in the case of MbCN the energies of the $^4A_2$ level and the $^6A_1$ level could not be determined very exactly because their contributions to the magnetizations $\langle M \rangle_T$ are very small. The results for myoglobin cyanide are summarized in Table 2.

Mössbauer Absorption Spectra

In Figures 6 and 7 the Mössbauer spectra taken for a metmyoglobin and a myoglobin fluoride sample, both in a 2.5 molar $(NH_4)_2SO_4$-solution, are shown. If the molarity of the buffer is much lower, the Mössbauer spectrum of $Mb(H_2O)$ at 4.2 K shows a second species of $Mb(H_2O)$, which might be a low spin compound. A comparison of the Mössbauer spectra of metmyoglobin solutions with high and low molarity is given in Figure 5. As the optical absorption spectra of these two samples at room temperature did not show any differences, we believe this second species of

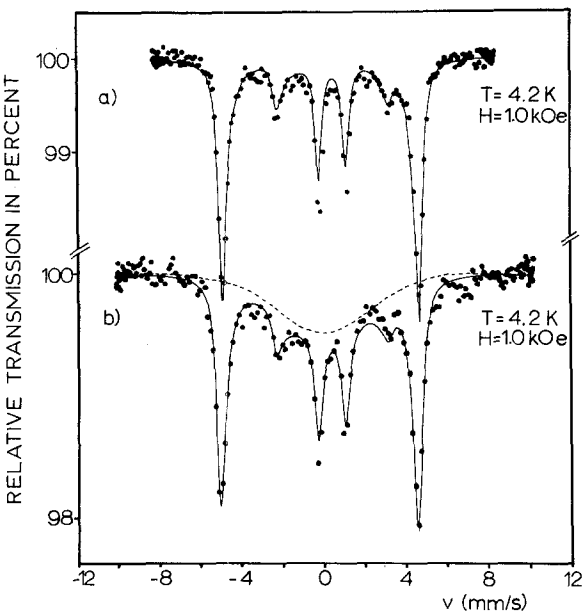

Fig. 5. Mössbauer spectra of $Mb(H_2O)$ at $T = 4.2$ K and at a longitudinal magnetizing field of $H = 1.0$ kOe. a) $Mb(H_2O)$ in a 2.5 molar $(NH_4)_2SO_4$ solution at pH = 6.3. b) $Mb(H_2O)$ in a 0.05 molar $(NH_4)_2SO_4$ solution at pH = 6.7. The dashed curve shows the part of the spectrum which is attributed to the low spin compound of $Mb(H_2O)$

metmyoglobin to be formed during the freezing of the solution. For least squares fitting of the spectra at $T = 4.2$ K and at low magnetizing fields $\vec{\mathbf{H}}$ we used six parameters. These are the isomer shift S (relative to the ^{57}Co in Rh source), the quadrupole splitting $\frac{1}{2} \cdot e \cdot Q \cdot V_{zz}$, the magnetic hyperfine interaction constant A_0, the linewidth Γ_{exp} and the maximum and minimum counting rates of the spectrum. The parameters S, $\frac{1}{2} \cdot e \cdot Q \cdot V_{zz}$ and A_0/β_n (β_n-nuclear magneton) for Mb and MbF, yielded by the least squares fits of the spectra of Figures 6 and 7 at $T = 4.2$ K are summarized in Table 3. As can be seen from Figure 5b we also fitted the spectrum of metmyoglobin, which had been prepared in a low concentrated buffer. We therefore simulated the spectrum of the low spin compound by means of a phenomenological curve proportional to the function $\frac{\pi}{2} \cdot \frac{v}{v_{max}}$.

The fitting parameters S, $\frac{1}{2} \cdot e \cdot Q \cdot V_{zz}$ and A_0/β_n of the spectrum of Figure 5b are within the indicated accuracy identical with that of the spectrum of $Mb(H_2O)$ in the high concentrated buffer (Fig. 5a).

As the relaxation times for MbF are longer as the ones for $Mb(H_2O)$ (compare Fig. 6 with Fig. 7), it has been possible to fit the Mössbauer spectrum of MbF at $T = 10$ K and $H = 1.0$ kOe. That spectrum is essentially composed of two different spectra, because at $T = 10$ K the two lowest Kramers doublets of the $^6A_1$ ground state have to be taken into account. By means of the Boltzmann distribution function we calculated the relative intensities of the two different Mössbauer spectra

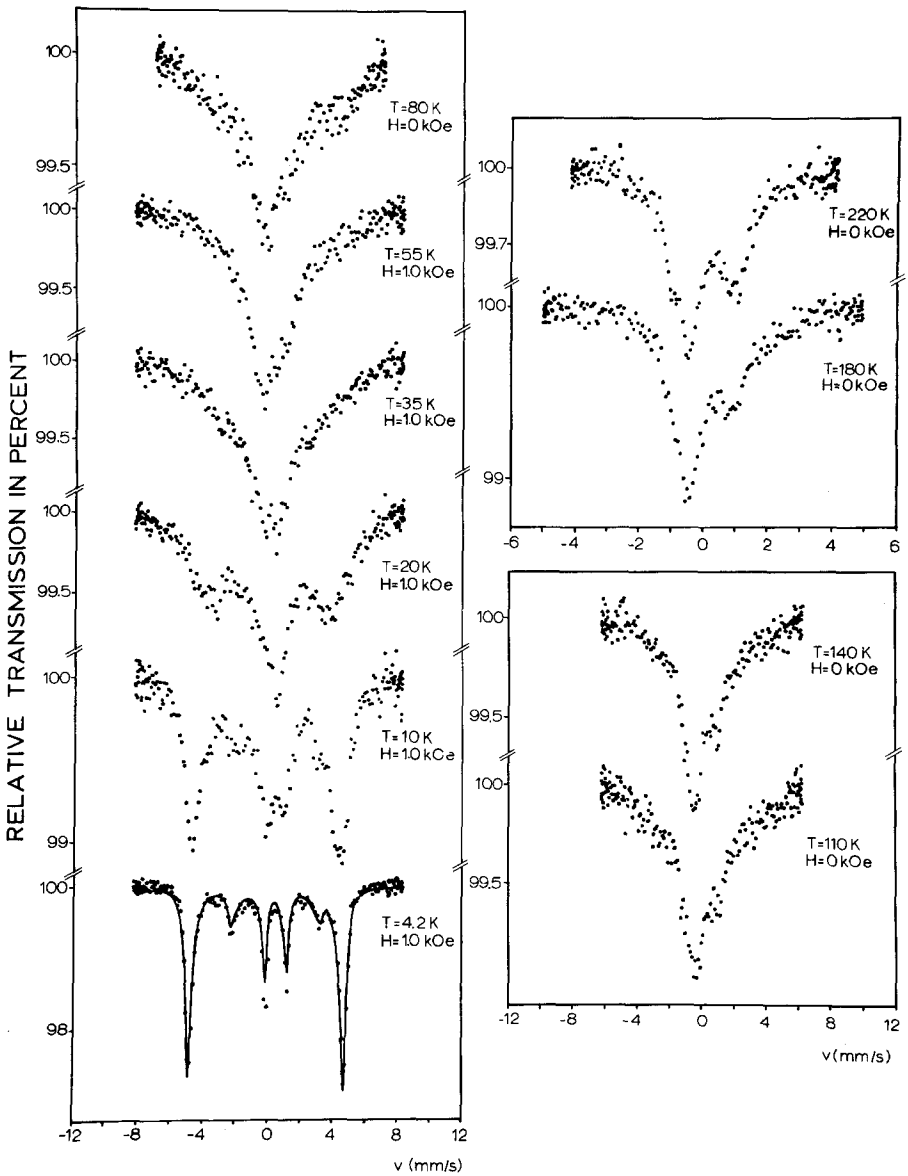

Fig. 6. Mössbauer spectra of $Mb(H_2O)$ in a 2.5 molar $(NH_4)_2SO_4$ solution (pH = 6.3) at different temperatures with or without a longitudinal magnetizing field $\vec{H}$.

produced by the two lowest Kramers doublets. Thereby we introduced a further parameter Δ_1, which is the energy difference of these two doublets. We took the values S, $\frac{1}{2} \cdot e \cdot Q \cdot V_{zz}$ and A_0, which were obtained from the fit of the spectrum at $T = 4.2$ K as constants. Then only four parameters determine the fit to the spectrum at $T = 10$ K. The least squares fitting procedure yielded for the energy $\Delta_1 = 14.0 \pm 1.5$ cm^{-1}.

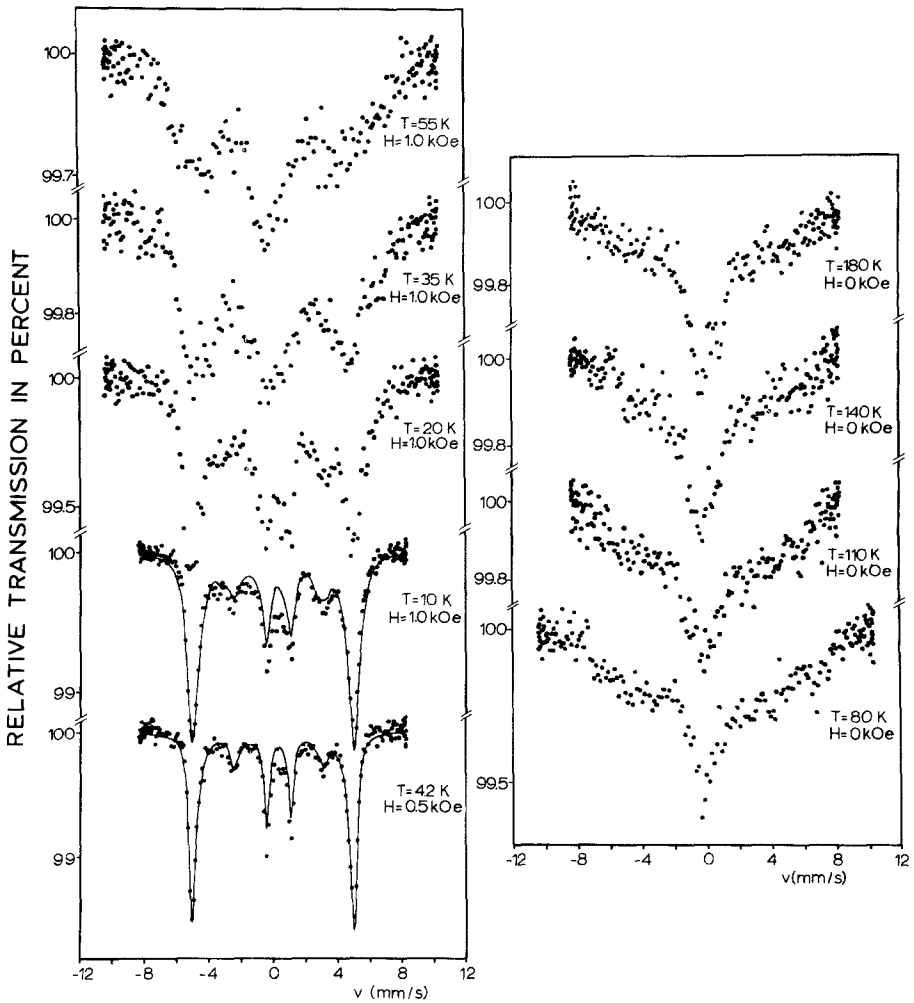

Fig. 7. Mössbauer spectra of MbF in a 2.5 molar $(NH_4)_2SO_4$ solution saturated with NaF (pH = 6.8) at different temperatures with or without a longitudinal magnetizing field $\vec{H}$.

Table 3. The fitting parameters S (isomer shift relative to a ^{57}Co in Rh source), $\frac{1}{2} \cdot e \cdot Q \cdot V_{zz}$ (quadrupole splitting), and $\frac{A_0}{\beta_n}$ (magnetic hyperfine interaction constant) of the Mössbauer spectra of $Mb(H_2O)$ and MbF at $T = 4.2$ K and low magnetizing fields $\vec{H}$. The spectra are shown in Figures 6 and 7

	$Mb(H_2O)$ (pH = 6.3)	MbF (pH = 6.8)
S [mm/s]	0.170 ± 0.01	0.172 ± 0.01
$\frac{1}{2} \cdot e \cdot Q \cdot V_{zz}$ [mm/s]	1.24 ± 0.04	0.77 ± 0.05
$\frac{A_0}{\beta_n}$ [kOe]	200.4 ± 0.4	211.4 ± 0.5

5. Discussion

Since experimental susceptibility data of $Mb(H_2O)$ and MbF measured at low temperatures have already been published earlier by Tasaki et al. (1967), it is possible to compare these data with our results. As may be seen by comparison with Figure 1 of Tasaki et al. (1967), similar results were obtained by us in the case of MbF. Our susceptibilities of $Mb(H_2O)$, however, are about 3–4% lower within the temperature region of $4.2\,K \leq T \leq 14\,K$. Above $T = 14\,K$ this difference vanishes. Since to our knowledge the temperature dependences of the magnetic susceptibility of $Mb(H_2O)_{p\text{-Ice}}$ and MbCN are not published, a comparison of these data is not possible. Only the induced effective magnetic moments of MbCN calculated from the susceptibilities at $T = 4.2\,K$ and at $T = 150\,K$ are given by Tasaki et al. (1967).

With the determination of the energies and the wave functions of the low-lying electronic levels we are able to calculate the molar susceptibility of $Mb(H_2O)$ and MbF at any temperature. In this way we compared calculated susceptibilities with experimental data collected at room temperature by Beetlestone et al. (1964) and by Theorell et al. (1951). No difference within the indicated accuracy were found and it can be concluded, that the electronic structures of $Mb(H_2O)$ and MbF determined at low temperatures in this work are identical with the ones existing at room temperatures.

In the field of Mössbauer spectroscopy spectra of $Mb(H_2O)$ and MbF at $T = 4.2\,K$ with an applied magnetizing field ($H \lesssim 10\,kOe$) had been published by Lang (1970). The spectrum of $Mb(H_2O)$ at $T = 4.2\,K$, however, had not been fitted by a theoretical curve. This might be due to the fact, that the sample used by Lang (1970) was not absolutely free of the low spin compound which appears, if the sample is prepared in a low molar salt solution. The fit of the MbF spectrum taken at $T = 4.2\,K$, where such a low spin compound is not to be seen, shows a very good agreement in comparison to our results. As has been shown in part 4 of this work, we could determine the energy difference Δ_1 of the two lowest Kramers doublets of the ${}^6A_1$-term of MbF fitting the Mössbauer spectrum at $T = 10\,K$ and $H = 1.0\,kOe$. To determine this energy Δ_1 Lang (1970) used the spectrum of MbF at $T = 4.2\,K$ and $H = 10.2\,kOe$. The evaluation of this spectrum was done by means of a Spin Hamiltonian with the crystal field parameter D($2 \cdot D$ corresponds to Δ_1). The energy $\Delta_1 = 14.0 \pm 1.5\ cm^{-1}$ yielded from our spectrum and the energy given by Lang (1970) $2 \cdot D = 12.6 \pm 1.0\ cm^{-1}$ are in agreement to each other.

The Mössbauer spectra of $Mb(H_2O)$ and MbF at temperatures $4.2\,K \leq T \leq 180\,K$ have not been published earlier. As may be seen from Figures 6 and 7 we could not fit the Mössbauer spectra of $Mb(H_2O)$ and MbF at temperatures $T > 10\,K$ to appropriate theoretical curves. An approach to a relaxation theory, which should be able to describe the spectra at higher temperatures is in progress. Nevertheless, a qualitative comparison of the spectra of $Mb(H_2O)$ and MbF (see Figures 6 and 7) shows, that in $Mb(H_2O)$ the relaxation times of the spin flips are shorter than in MbF. One may assume, that the spin flips are caused by spin lattice relaxations. Since the electron spins are coupled to the phonons via spin orbit coupling, the difference of the relaxation times become understandable: the off-diagonal matrix elements of the Hamiltonian describing the spin-orbit coupling between the

$^6A_1$ and the $^4A_2$ level are inverse proportional to the energy difference between these two levels. Therefore one should expect, that the energy of the $^4A_2$ level relative to the $^6A_1$ ground state in $Mb(H_2O)$ is lower than in MbF, which is in agreement with our results of the susceptibility data.

A comparison between our results and the results, which were obtained by other spectroscopic methods is possible only in a limited way. Examples are the determination of the anisotropy of the magnetic susceptibility of single crystals by Morimoto et al. (1965) and by Uenoyama et al. (1968) and far infrared spectroscopic data by Brackett et al. (1971). These data have all been evaluated using a Spin Hamiltonian. Therefore only a comparison of the energy Δ_1 as obtained from our evaluations with the crystal field parameter $2 \cdot D$ of the Spin Hamiltonian is possible. A fairly good agreement is obtained. It should be mentioned, however, that the determination of the energy $2 \cdot D$ by far infrared spectroscopy is of poor accuracy in the region of $2 \cdot D > 16\ cm^{-1}$. The evaluations of the magnetic field dependence of the EPR data as given by Gray et al. (1973) and by Slade et al. (1972) also using a Spin Hamiltonian gave larger deviations between Δ_1 and $2 \cdot D$. These discrepancies may arise from the fact, that the treatment of the data does not correctly consider the mixing of the different Kramers doublets of the $^6A_1$ level due to the strong magnetizing fields $\vec{\mathbf{H}}$. A new evaluation which was done by Eicher (1975), showed, that the agreement to our results became much better. In these calculations of these EPR data, Eicher (1975) used the susceptibilities of $Mb(H_2O)$ and MbF at temperatures $4.2\ K \leq T \leq 20\ K$ measured by Tasaki et al. (1967). Therefore the results for MbF agree very good with our results, whereas in the case of $Mb(H_2O)$ some differences are to be seen. It should be added that to our opinion the error bars of the energies of the electronic levels given by Eicher (1975) are too small, because the uncertainty of the energy ε_1 has not been taken into account.

Finally we want to discuss the structural significance of the results for the splitting energies of the antibonding single $3d$ electron orbitals d_{z^2} and $d_{x^2-y^2}$ relative to the d_{xy}-orbital designed by ε_2 and ε_3 (see Fig. 1). It is easy to understand, that the energy of the antibonding $d_{x^2-y^2}$ orbital ε_3 has to increase, if the bonding of the iron ion to the four nitrogen atoms of the protoporphyrin ring system becomes stronger. That means, the overlap between the $d_{x^2-y^2}$ orbital and the wave functions of the nitrogen atoms with σ-bonding character becomes larger. Therefore one expects that the energy ε_3 increases, if the distance between the iron ion and the protoporphyrin ring plane becomes smaller. Accordingly the energy ε_2 has to increase, if the distance between the iron and its axial ligands decreases. The comparison of $Mb(H_2O)$ with $Mb(H_2O)_{p\text{-Ice}}$ shows that not only ε_2 but also ε_3 of $Mb(H_2O)_{p\text{-Ice}}$ exceeds the corresponding energies of $Mb(H_2O)$. Therefore one may conclude, that by the application of the hydrostatic pressure of 2500 atm the nitrogen atom N_ϵ of the proximal histidine F8 in $Mb(H_2O)_{p\text{-Ice}}$ is moved towards the iron, which thereby is pushed to the porphyrin ring plane. The comparison of $Mb(H_2O)$ and MbF shows that in $Mb(H_2O)$ the iron is placed nearer to the porphyrin ring plane than in MbF. A comparison of the energies ε_2 of $Mb(H_2O)$ and MbF in this way gives no clear result, since the ligands at the sixth coordination position of the iron are different. It is not known how much ε_2 will be influenced by this. The distance of the iron to the porphyrin ring plane in MbCN proved to be the shortest in comparison to the high spin compounds, because the

energy ε_3 clearly exceeds the corresponding energies ε_3 of the high spin compounds.

The energies ε_2 and ε_3 of the ferrous iron in myoglobin ($\varepsilon_{2,\ Fe^{2+}-Mb} = 7900$ cm^{-1}, $\varepsilon_{3,\ Fe^{2+}-Mb} = 17270$ cm^{-1}) have already been published by Eicher et al. (1975). A comparison between the spatial arrangement of the ferrous iron and the ferric iron may also be derived. It is obvious, that the ferric iron lies closer to the porphyrin ring plane than the ferrous iron ($\varepsilon_{3,\ Fe^{3+}-Mb(H2O)} > \varepsilon_{3,\ Fe^{2+}-Mb}$), which is qualitatively in good agreement with the structural considerations of Perutz (1970). The differences of the energies ε_2 of the ferrous and the ferric iron may to some extent result from the additional axial ligand (H_2O-molecules) of the ferric iron in metmyoglobin. A more detailed discussion about the energy ε_2 is not indicated with the set of data presently available.

Acknowledgements. These investigations were supported by the Deutsche Forschungsgemeinschaft. We gratefully acknowledge the assistance of B. Wintergerst in the biochemical preparations. We thank Prof. K. Gersonde for helpful discussions.

References

Antonini, E., Brunori, M.: Hemoglobin and myoglobin in their reactions with ligands, chap. 3: The derivatives of ferric hemoglobin and myoglobin. Amsterdam-London: North-Holland 1971

Beetlestone, J., George, P.: A magnetochemical study of equilibria between high and low spin states of metmyoglobin complexes. Biochemistry **3,** 707–714 (1964)

Brackett, G. C., Richards, P. L., Caughey, W. S.: Far infrared magnetic resonance in Fe (III) and Mn (III) porphyrins, myoglobin, hemoglobin, ferrichrome A and Fe (III) dithiocarbonates. J. Chem. Phys. **54,** 4383–4401 (1971)

DeBennedetti, S.: Nuclear interactions, p. 259. New York: Wiley 1964

DeDuve, C.: A spectrophotometric method for the simultaneous determination of myoglobin and hemoglobin in extracts of human muscle. Acta Chem. Scand. **2,** 264–289 (1948)

Eicher, H., Trautwein, A.: Electronic structure and quadrupole splitting of ferrous iron in hemoglobin. J. Chem. Phys. **50,** 2540–2551 (1969)

Eicher, H., Bade, D., Parak, F.: Theoretical determination of the electronic structure and the spatial arrangement of ferrous iron in deoxygenated sperm whale myoglobin and human hemoglobin from Mössbauer experiments. J. Chem. Phys. **64,** 1446–1455 (1976)

Eicher, H.: Electronic structure and spatial arrangement of C_{2v} coordinated ferric iron in metmyoglobin, metmyoglobin fluoride and methemoglobin. Z. Naturforsch. **30c,** 701–710 (1975)

Feldmann, D., Hunt, R. P.: Vibrationsmagnetometer, Überblick und Stand der Entwicklung. Z. Instr. **72,** 259–265 (1964)

Frauenfelder, H.: Dynamics of biomolecules. Proc. Int. Conf. on Mössbauer spectroscopy, vol. 2 (ed. A. Z. Hrynkiewicz, J. A. Sawicki), pp. 305–317. Cracow 1975

Gray, A. L., Buckmaster, H. A.: Electron paramagnetic resonance (34 and 55 GHz) studies of hemoproteins. Canad. J. Biochem. **51,** 1142–1153 (1973)

Horrocks, W. DeW., Jr., Greenberg, E. S.: Isotropic nuclear magnetic resonance shifts in low spin iron (III) porphyrin and hemin systems. Theoretical interpretation of temperature dependences. Mol. Phys. **27,** 993–999 (1974)

Kaindl, G., Maier, M. R., Schaller, H., Wagner, F.: A Mössbauer spectrometer for the measurement of small isomer shifts. Nucl. Instr. Meth. **66,** 277–282 (1968)

Kendrew, J. C., Parrish, R. G.: The crystal structure of myoglobin III. sperm whale myoglobin. Proc. Roy. Soc. **A238,** 305–324 (1957)

Lang, G.: Mössbauer spectroscopy of haem proteins. Quart. Rev. Biophys. **3,** 1–60 (1970)

Morimoto, H., Jizuka, T., Otsuka, J., Kotani, M.: Magnetic anisotropy of the myoglobin single crystal. Biochim. Biophys. Acta **102,** 624–625 (1965)

Parak, F., Formanek, H.: Untersuchung des Schwingungsanteils und des Kristallgitterfehleranteils des Temperaturfaktors in Myoglobin durch Vergleich von Mössbauerabsorptionsmessungen und Röntgenstrukturdaten. Acta Cryst. **A 27,** 573–578 (1971)

Parak, F., Weber, E., Thomanek, F., Steigemann, W.: X-ray structure investigations of sperm whale myoglobin at 77 K (meeting abstract). Acta Cryst. **A 31,** 300–300 (1975)

Perutz, M. F.: Stereochemistry of cooperative effects in haemoglobin. Nature **228,** 726–739 (1970)

Perutz, M. F., Ladner, J. E., Sanford, R. S., Chien Ho: Influence of globin structure on the state of the heme. I. Human deoxyhemoglobin. Biochemistry **13,** 2163–2173 (1974)

Perutz, M. F., Fersht, A. R., Sanford, R. S., Roberts, G. C. K.: Influence of globin structure on the state of heme. II. Allosteric transitions in methemoglobin. Biochemistry **13,** 2174–2186 (1974)

Perutz, M. F., Heidner, E. J., Ladner, J. E., Beetlestone, J. G., Chien Ho, Slade, E. F.: Influence of globin structure on the state of heme. III. Changes in heme spectra accompanying allosteric transitions in methemoglobin and their implications for heme-heme interaction. Biochemistry **13,** 2187–2200 (1974)

Slade, E. F., Farrow, R. H.: Millimeter wave EPR studies of some high spin myoglobin derivatives. Biochim. Biophys. Acta **278,** 450–458 (1972)

Tasaki, A., Otsuka, J., Kotani, M.: Magnetic susceptibility measurements on hemoproteins down to 4.2 K. Biochim. Biophys. Acta **140,** 284–290 (1967)

Theorell, H., Ehrenberg, A.: Spectrophotometric, magnetic and titrimetric studies on the heme linked groups in myoglobin. Acta Chem. Scand. **5,** 823–853 (1951)

Thomanek, U. F., Parak, F., Mößbauer, R. L., Formanek, H., Schwager, P., Hoppe, W.: Freezing of myoglobin crystals at high pressure. Acta Cryst. **A 29,** 263–265 (1973)

Trautwein, A.: Mössbauer spectroscopy on heme proteins. Structure and bonding, vol. 11, pp. 101–167. Berlin-Heidelberg-New York: Springer 1975

Uenoyama, H., Jizuka, T., Otsuka, J., Kotani, M.: Paramagnetic anisotropy measurements on acid ferrimyoblogin and ferrimyoglobin fluoride. Biochim. Biophys. Acta **160,** 159–166 (1968)

Received February 3, 1976/Accepted February 11, 1977